A Rear-End Collision Avoidance Scheme for Intelligent Transportation System

Chen Chen[1] , Hongyun Liu[1], Hongyu Xiang[1], Meilian Li[1], Qingqi Pei[1] and Shengda Wang[2]

[1]*State Key Laboratory of Integrated Service Networks Xidian University, Xi'an 710071, China*
[2]*Jilin Electric Power Company Limited Communication Branch Transport Department, Changchun 130021, China*

Abstract. In this paper, a rear-end collision control model is proposed using the fuzzy logic control scheme for the autonomous or cruising vehicles in Intelligent Transportation Systems (ITSs). Through detailed analysis of the car-following cases, our controller is established on some reasonable control rules. In addition, to refine the initialized fuzzy rules considering characteristics of the rear-end collisions, the genetic algorithm is introduced to reduce the computational complexity while maintaining accuracy. Numerical results indicate that our Genetic algorithm-optimized Fuzzy Logic Controller (GFLC) outperforms the traditional fuzzy logic controller in terms of better safety guarantee and higher traffic efficiency.

1 Introduction

According to the investigations and statistics, of all the traffic accidents that ever took place, about 60 to 70 percent were caused by vehicle collisions, particularly rear-end collisions [1]. To alleviate the growing risks of rear-end collisions, the auxiliary or automatic control methods proposed for autonomous or cruising vehicles in ITSs look promising. Actually, there have been many classic automatic control schemes proposed, such as PID control [2], sliding mode control [3], and the linear quadratic optimal control [4]. Although these methods enable accurate control to be exercised, they are highly dependent on precise mathematical models. In practice, an accurate control model for vehicle collision avoidance is almost unavailable.

Instead of precise control, the fuzzy logic-based controllers (FLC) are also well studied to reduce the possible vehicle collisions in the last few years. Due to its superiority in solving problems in multi-parameter, non-linear systems as well as capturing the driving characteristics in a vehicular environment, it is feasible and preferable to apply FLC-related models to vehicular active control issues. However, since the effect of a FLC relies on the number of fuzzy rules, an excessive number of such will directly impair its effectiveness. Moreover, the number of fuzzy rules increases exponentially with the number of fuzzy subsets, resulting in greater computational complexity of the controller. Among various schemes that have been proposed to address the above-mentioned problems and have become an active research topic recently is combining neural network (BP) with fuzzy control [5, 6]. However, the neural network converges slowly and is prone to being stuck in local optimum. Unlike the neural network, the genetic algorithm (GA) is capable of searching for the global optimal solution and is almost application-independent. To efficiently reduce the risk in car-following scenario, this paper proposes a rear-end collision avoidance system that uses the fuzzy logic control model with its fuzzy rules optimized by the generic algorithm. This GA-based FLC should be able to allow drivers to promptly avoid approaching risks and accurately make a brake, as well as accommodating driving behaviours of drivers. In addition, the model is also applicable to the popular autonomous vehicles or vehicles in cruising state to keep a safe inter-vehicle space and at the same time improve the driving efficiency by controlling the headway.

2 GA-based FLC

In practical cases, the factors that influence driving safety are very complicated and usually include weather conditions, road surface situations, response time of drivers, vehicle dynamics, etc. Since most of these factors are non-linear and time-varying, obtaining an accurate mathematical model of the vehicle control system is difficult. In this context, some of the traditional methods (e.g., PID control, linear quadric-form optimal control) are unable to exercise accurate control. On the other hand, fuzzy control has advanced considerably in control and reason applications in recent years mainly due to its independence from accurate mathematical models. Its performance relies on the number of fuzzy rule bases, the number of linguistic variables as well as the types and ranges of membership functions. An excessive number of fuzzy control rule bases and linguistic variables results in longer FLC search time and higher computational

complexity. Therefore, the key to FLC design is to determine the fuzzy control rule base and input/output membership function, which are usually acquired by expert summarization. However, in practical applications, an FLC generally cannot always guarantee its effectiveness, highlighting the need for optimization. By reviewing previous studies, there are many optimization schemes that optimize fuzzy control rules [7-9] or the input/output quantified scale factors [10]. In this paper, GA is used to optimize the control rules by finding the optimal input/output variables combination. The flowchart of our proposed GA-based FLC to avoid the rear-end collisions in car-following scenarios is shown in Fig. 1.

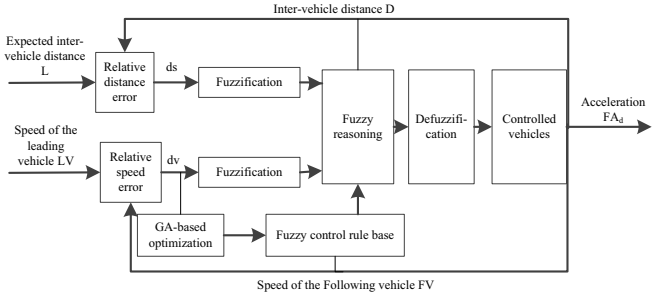

Figure 1. GA-based FLC.

To exercise effective control over vehicles, a dual-input single-output fuzzy controller is designed as Fig. 1 illustrates. The relative distance error ds and the relative speed error dv between the leading and trailing vehicles are defined as the input variables. The output acceleration FA_d is defined as the output variable. The input variables are given as

$$ds = D - S, \tag{1}$$

$$dv = LV - FV, \tag{2}$$

where D denotes the inter-vehicle distance, S denotes the expected inter-vehicle space, LV and FV are the speeds of the leading and trailing vehicles, respectively. Note that D here denotes the current longitudinal inter-vehicle distance measured using such as line laser [11] or wireless signal [12] while S indicates the inter-vehicle space by which the driving safety could be guaranteed considering the vehicular dynamics and braking process. The speed of the trailing vehicle FV should be known since the collision warning system has been installed on it, while the speed of the leading vehicle LV could be obtained through GPS sharing [13] or wireless communication systems.

2.1 Fuzzification of input/output variables

In our work, the ranges of the input/output variables are properly set based on practical considerations. According to the braking distance algorithm from Mazda[14], we have:

$$S = \frac{1}{2}\left(\frac{FV^2}{a_{-\max}} - \frac{LV^2}{a_{-\max}}\right) + FV \cdot \tau_1 + dv \cdot \tau_2 + d_0, \tag{3}$$

where τ_1 and τ_2 denote the delay. d_0 denotes the distance between the two vehicles after they stop. Generally, $\tau_1 = 0.1s$, $\tau_2 = 0.6\text{s}$, and $d_0 = 1.5m$, where τ_1, τ_2 and d_0 are the system delay, driver reaction time and minimum distance needed to prevent a collision if both vehicles begin braking with their respective maximum decelerations, respectively. In the case of the leading vehicle braking immediately at a speed of 120km/h (i.e., 33.33m/s), the expected inter-vehicle space is 67.5m. So the relative distance error is set from -67.5m to 67.5m. According to the Chinese-laws on the speedway[15], vehicles drive at a speed varying from 60km/h to120km/h, so the range of dv in our work is [-60km/h, 60km/h]. Taking into account the comfort of drivers and passengers, the acceleration of the trailing vehicle is set to [-8m/s^2, 8m/s^2].

The relative distance error ds, relative speed error dv and acceleration FA_d are first fuzzified into seven fuzzy subsets: negative large (NL), negative medium (NM), negative small (NS), zero (Z), positive small (PS), positive medium (PM), and positive large (PL). Before the fuzzification, scaling transformations need to be made to the actual input variables such that they can be transformed into the specified domains. Therefore, we have

$$x_0 = \frac{x_{\min} + x_{\max}}{2} + k\left(x_0^* - \frac{x_{\min}^* + x_{\max}^*}{2}\right), \tag{4}$$

$$k = \frac{x_{\max} - x_{\min}}{x_{\max}^* - x_{\min}^*}, \tag{5}$$

where x_0^* denotes the actual input variable, $\left[x_{\min}^*, x_{\max}^*\right]$ denotes the range of the variable, $\left[x_{\min}, x_{\max}\right]$ denotes the specified domain of the variable and k denotes the scaling factor. For the relative distance error ds, the scaling factor $k_1 = 0.05$. Using Equation (4), it can be determined that the fuzzy domain of the relative distance error is [-6, 6]. Since the range of the relative speed error dv is [-16.67m/s, 16.67m/s] and the scale factor $k_1 = 0.36$, the fuzzy domain of the relative speed error is [-6, 6] by (4). Similarly, since acceleration FA_d is limited to [-8m/s^2, 8m/s^2] and the scale factor $k_1 = 0.75$, its fuzzy domain is [-6, 6].

2.2 Determination of membership functions

In our work, the triangle function is used as the membership functions for the relative distance error ds, the relative speed error dv and the acceleration FA_d. The domain of each linguistic variable is partitioned into seven parts for ds, dv and FA_d as shown in Fig. 2

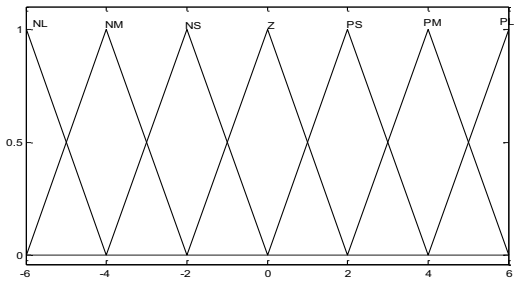

Figure 2. Membership function of ds , dv and FA_d .

2.3 Establishment of the fuzzy rules

To construct the fuzzy rules used to control the risky vehicles when a specific condition is met, the experience of drivers should be fully considered. According to the common response for a normal person, the following typical driving scenarios are taken into account:

(1) If the inter-vehicle distance is small and the speed of the trailing vehicle is substantially larger than that of the leading vehicle, then rear-end collision has a high probability of occurrence. In this case, the trailing vehicle should brake immediately to decelerate for collision avoidance.

(2) If the inter-vehicle distance is still large and the speed of the trailing vehicle is close to that of the leading vehicle, then rear-end collision has a small probability of occurrence. In this case, the speed of the trailing vehicle can remain or increase properly.

(3) If the inter-vehicle distance is small and the speed of the trailing vehicle is close to that of the leading vehicle, then the driver of the trailing vehicle should brake slightly in order to prevent rear-end collision and ensure driving safety.

Based on above driving experiences as well as trial-and-error, a set of 49 rear-end avoidance fuzzy control rules representing the actual driving experience is devised and shown in Table 1. The g^{th} rule R^g is:

$$if\ x_{ds}\ is\ A^g\ and\ x_{dv}\ is\ B^g\ then\ y_{FA_d}\ is\ C^g, \tag{6}$$

where x_{ds} is the input value of ds , x_{dv} is the input value of dv , y_{FA_d} is the output value, A^g and B^g denote the fuzzy subsets of ds and dv , respectively. C^g denotes the fuzzy subset of FA_d . The fuzzy rule R^g can be regarded as the fuzzy implication $A^g \times B^g \to C^g$ over the product space $U_{fz} \times V_{fz}$, where $U_{fz} = A^g \times B^g$.

Table 1. Fuzzy control rules for the real-end avoidance system.

Control variable		Relative distance error						
		NL	NM	NS	Z	PS	PM	PL
relative speed error	NL	NL	NL	NL	NM	NM	NS	NS
	NM	NL	NL	NM	NM	NS	NS	Z
	NS	NL	NM	NS	NS	NS	Z	Z
	Z	NM	NS	Z	NS	Z	PS	PS
	PS	NM	Z	Z	Z	Z	PM	PL
	PM	NS	Z	Z	PS	PM	PL	PL
	PL	NS	Z	Z	PS	PL	PL	PL

2.4 Optimizing to the fuzzy rules using genetic algorithm

The fuzzy rules determined in the previous subsection will be optimized with the genetic algorithm to reduce the problem scale of our collision control strategy. The detailed steps are given as follows:

2.4.1 Coding of the fuzzy control rule

To optimize the fuzzy rules, we first encode it using the binary coding scheme [15]. Each rule is represented by four binary numbers, the first of which is the control bit and the other three are the rule representation bits. The tandem coding method is employed by connecting these 49 rules to form a chromosome. According to our predefined fuzzy rules, these 49 rules will be the parameters to be optimized. The antecedents of the rules are ds and dv , and the consequent is FA_d . Because the control variable has seven fuzzy sets, the consequent of the rules can be represented via three-digit binary coding, i.e., 000, 001, 010, 011, 100, 101 and 110. If a certain fuzzy rule does not exist, then let X denote the consequent of the rule and its code is 111. Thus, the 49 control rules in Table 1 can be numbered as rule1 to rule49, sequentially. Next, the above 49 rules can be connected in a tandem manner to provide the chromosome of the rules as shown in Fig.3. The chromosome of the rules is the unit of the population, i.e., the operand of GA. Each bit of the control gene controls the corresponding rule. As a result, the GA-based optimization yields the fuzzy rules consisting of fewer but more effective rules.

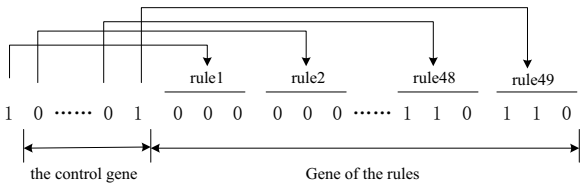

Figure 3. Chromosome of the rules

2.4.2 Determination of the fitness function

Since our FLC is designed to avoid rear-end collisions, the key to achieving this objective is to ensure both the relative distance error ds and the relative speed error dv are small. Therefore, the objective function J is defined as:

$$J = |ds| + |dv|. \tag{7}$$

It is worth noting from (8) that the smaller the value of J , the better the performance of our FLC. However, generally, the GA prefers individuals with high fitness. So, our objective function needs to be properly transformed into a fitness function, which is given by:

$$f = \frac{1}{1+J}. \tag{8}$$

2.4.3 Determination of the genetic parameters

The effectiveness of the GA relies on the related genetic parameters, including the population size n, the crossover probability P_c and the mutation probability P_m. Usually, the large size of the initial population means a high space and time complexity. The size of the initial population is usually within the range [20,100] [16]. In our work, the initial population is obtained in the following way:

a) Randomly extract 80 matrixes with 7 rows and 7 columns as the matrixes of the control variables. Elements of all matrixes are integers ranging from 1 to 7.

b) Compute the fitness f of each individual, and sort these n individuals in descending order of f.

c) Eliminate m=30 individuals with small fitness, define the remaining individuals as the initial population S1, thereby obtaining an initial population whose size $n_{s1} = 50$.

Note that each individual represents a chromosome of the rules. In this paper, the crossover probability P_c is 0.7. Because a small mutation probability P_m can effectively prevent damage to the good individuals, P_m is set to 0.001. The number of iterations is set to G=30.

2.4.4 Determination of selection, crossover and mutation operations

Biological evolution is achieved via genetic operations. Therefore, genetic operators are essential for optimization of fuzzy rules.

a) Selection operator. The fitness proportional selection operator is used. The fitness is first calculated using the fitness function and then the replication probability of each individual is obtained. The number of replications of this individual in the next generation is equal to the product of the replication probability and the population size. The probability P_{si} that each individual is selected is denoted by:

$$P_{si} = \frac{f_i}{\sum_{j=1}^{n_{s1}} f_j}, \tag{9}$$

where n_{si} is the population size, and f_i is the fitness of the i^{th} individual in the population.

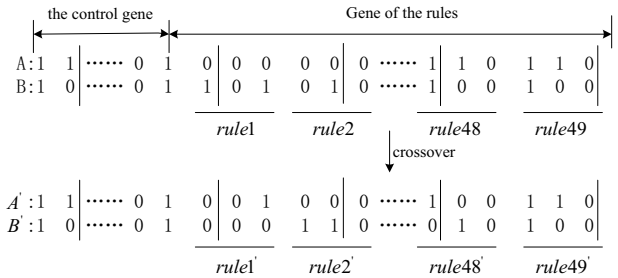

Figure 4. Illustration of the crossover operation.

b) Crossover operator. During the crossover operation, the chromosomes before the cross point undergo the mutation operation, while those after the cross point undergo crossover and mutation operations. The crossover probability $P_c = 0.7$, and the crossover operation is illustrated in Fig. 4.

c) Mutation operator. The basic-bit mutation method is used in our work. Because binary coding is carried out on the fuzzy control rules, the mutation operator may involve reversing genes of some gene bits (e.g., $0 \to 1$ or $1 \to 0$). The mutation probability $P_m = 0.001$. Note that the mutation operations improve the local search ability of GA and avoid premature convergence.

Finally, through the GA optimization, the number of the fuzzy rules has been reduced from 49 to 28.

2.5 Defuzzification of the output variables

The defuzzification process takes the fuzzy sets and produces a single-value output. In our paper, the control variable is defuzzified via the gravity method as:

$$Y_{out} = \frac{\sum_{g=1}^{7} l \cdot \eta_{C^g}(l)}{\sum_{g=1}^{7} \eta_{C^g}(l)}, \tag{10}$$

where l, as we have stated before, is the value of the output in the domain, $\eta_{C^g}(l)$ is the membership of l with respect to the fuzzy set C^g.

3 Simulations

To demonstrate the superiority of our GFLC controller, both FLC and GFLC are simulated under typical car-following scenarios. The simulation setup is as follows: the sampling time is 0.1s, total simulation time is 80s, initial distance between two vehicles is 20m, the initial speeds of the leading and trailing vehicles are 20m/s and 30m/s, respectively. Note that in our simulation, dv is initially set to -10m/s to increase the possibility of rear-end collision. The leading vehicle keeps a constant speed before 20s and then accelerates at 1m/s^2 during 20-30s. During 31-33s, the leading vehicle begins to brake at 4m/s^2. Note that the risk of rear-end collision with this configuration is very high between the leading and trailing vehicles, so that the trailing vehicle ought to brake immediately to avoid the collision. To obtain the statistical average, each test is repeated 30 times.

From Fig. 5, it can be observed that both controllers instruct the trailing vehicle to brake during the early period of the simulation for rear-end collision avoidance. However, it is worth noting that there is actually a slight difference between two controllers. GFLC executes the decelerate action from approximately seconds 30 while FLC at about seconds 32. This difference verifies that our controller has a better response speed to the possible dangers than FLC. In addition, during 20-30s, when the leading vehicle accelerates at 1m/ s^2, GFLC instructs the trailing vehicle to gradually increase the acceleration from approximately 0.1m/s^2 at 20s to almost 1m/s^2 at 30s. On the contrary, the FLC shows a fluctuant process

which first makes the acceleration increase from 0.28m/s^2 at 20s to 0.9m/s^2 at about 23s, and then suddenly decrease to almost 0.5m/s^2 at 30s. This dramatic variation implies that the rules used in the traditional FLC are unreasonable to some extent while our rules, optimized by GA, are well suited for the car-following scenario. During 31-33s, when the leading vehicle begins to decelerate with 4m/s^2, GFLC immediately outputs a deceleration for the trailing vehicle of about 4m/s^2 (equal to the deceleration of the leading vehicle), thus reducing the collision risk. However, FLC outputs a smaller deceleration which is actually insufficient to promptly avoid the possible rear-end collision. During 34-80s, since the rear-end collision risk is low, our GFLC almost keeps a zero acceleration for the trailing vehicle. However, during this period, FLC still yields non-zero accelerations which vibrate around 0m/s^2.

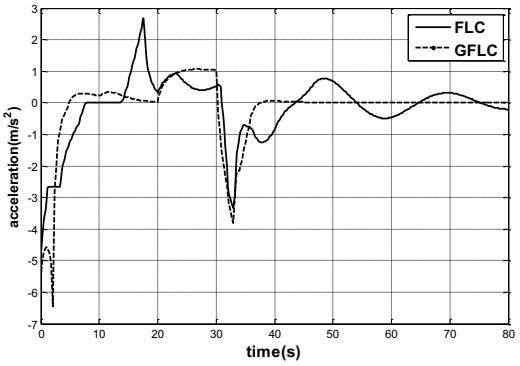

Figure 5. Comparison for accelerations of the trailing vehicle.

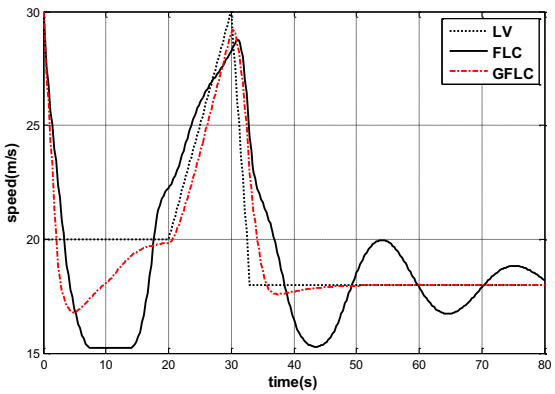

Figure 6. Comparison for transient speed of the trailing vehicle.

The transient speed comparisons between two models are depicted in Fig. 6. It can be observed that the leading vehicle keeps a steady speed before 20s while the trailing vehicle adapts itself according to the instructions of the corresponding controllers to avoid collision. It is worth noting that approximately before 8s, FLC outputs continuous deceleration for the trailing vehicle while GFLC outputs a rapid decrease before about 5s and then an increase during approximately 5-8s. Actually, since the *dv* is initially set to -10m/s, the trailing vehicle will reduce the gap to zero between two vehicles after 2 seconds. Under such circumstance, our GFLC first outputs a deceleration to avoid the possible collision in advance. After a continuous deceleration before about 5s, the inter-vehicle distance returns to a safe level and then a persistent acceleration has been given out by our GFLC till about 20s. In comparison, FLC instructs the trailing vehicle to drive at a very low speed, i.e., about 16m/s, during approximately 8-14s, which seems to overestimate the risk and result in a lower driving efficiency. During 20-30s, due to the acceleration of the leading vehicle, both controllers suggest a fast speed-up for the trailing vehicles. However, by checking the points carefully, it has been determined that our GFLC outputs more precise controlling instructions which are almost strictly consistent with our simulation configurations. On the contrary, FLC instructs the trailing vehicle to accelerate too fast for too long, say about 14-32s. During 31-33s of simulation, GFLC instructs the trailing vehicle to decelerate as soon as the leading vehicle decelerates, effectively avoiding the possible rear-end collision. With FLC, the trailing vehicle's speed changes slowly, thus increasing the rear-end collision risk. During 34-80s, GFLC enables the trailing vehicle to drive at a stable rate of 18m/s, reducing the risk and at the same time improving the driving efficiency. With FLC, it shows great fluctuation indicating the instability of its adopted fuzzy rules.

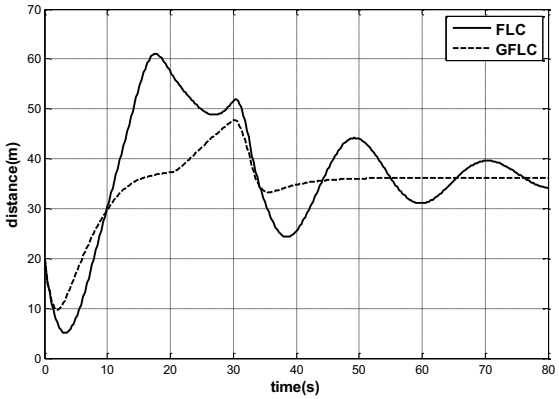

Figure 7. Comparison of inter-vehicle distance.

From Fig. 7, it can be observed that the inter-vehicle distance actually changes with the variation of acceleration. With GFLC, the inter-vehicle distance changes slightly during the entire simulation procedure and almost remains the same during 40-80s. In contrast, FLC causes continuous fluctuations. At about 4s, FLC even outputs an inter-vehicle distance of no more than 6 meters, which greatly increases the rear-end collision risk. Similarly, FLC also gives out a very large value, i.e., over 60 meters around 18s, which is really unnecessary considering the previous continuous low speed of the trailing vehicle. It is also worth noting that the lasting duration of inter-vehicle distance over 40 meters exceeds approximately 27s for FLC while it is only about 9s for our GFLC. This large difference confirms once again that GFLC is more effective than FLC in terms of driving efficiency.

4 Conclusions

In this paper, a novel fuzzy controller is proposed, which leverages GA to optimize the fuzzy control rules, to

improve the performance on rear-end collision avoidance of the vehicular control system, and enhances the emergency response ability. Simulation results successfully indicate that the proposed controller outperforms the traditional one and is capable of avoiding the possible rear-end collision while increasing the traffic efficiency.

Our future work will attempt to incorporate the advanced sensor system into our vehicular dynamics control framework and propose an effective active-control system. This could further reduce collision risks by introducing precise prediction algorithm depending on the online data collection module.

Acknowledgement

This work was supported by the National Natural Science Foundation of China (61201133, 61571338), the National Science and Technology Major Project of the Ministry of Science and Technology of China(2015zx03002006-003), the Natural Science Foundation of Shaanxi Province(2014JM2-6089), the National High-tech R&D Program of China (863 Program-2015AA015701), the Research collaboration innovation program of Xi'an(BD31015010001), the Hong Kong, Macao and Taiwan Science and Technology Cooperation Special Project (2014DFT10320, 2015DFT10160) and the “111 Project” of China (B08038).

References

1. S. H. Kim, P. S. Moon, W. S. Jang, K. S. Kim, S. C. Lee, M. Woo*, et al.*, "An experimental investigation of a CW/CA system for automobiles," SAE Technical Paper, (1999)
2. S. Moon, I. Moon, and K. Yi, "Design, tuning, and evaluation of a full-range adaptive cruise control system with collision avoidance," *Control Engineering Practice,* **17**, pp. 442-455, (2009)
3. A. Ferrara and C. Vecchio, "Second order sliding mode control of vehicles with distributed collision avoidance capabilities," *Mechatronics,* vol. 19, pp. 471-477, (2009)
4. J. van den Berg, D. Wilkie, S. J. Guy, M. Niethammer, and D. Manocha, "LQG-obstacles: Feedback control with collision avoidance for mobile robots with motion and sensing uncertainty," in Robotics and Automation (ICRA), 2012 IEEE International Conference on, pp. 346-353, (2012)
5. Y. J. Mon and C. M. Lin, "Supervisory recurrent fuzzy neural network control for vehicle collision avoidance system design," Neural Computing and Applications, **21**, pp. 2163-2169, (2012)
6. N. B. Hui, V. Mahendar, and D. K. Pratihar, "Time-optimal, collision-free navigation of a car-like mobile robot using neuro-fuzzy approaches," Fuzzy Sets and Systems, **157**, pp. 2171-2204, (2006)
7. H. S. Hwang, Y. H. Joo, H. K. Kim, and K. B. Woo, "Identification of fuzzy control rules utilizing genetic algorithms and its application to mobile robots," Algorithms and Architectures for Real-Time Control (Korea, 1992), pp. 249-254, (2014)
8. A. Jalali, F. Piltan, A. Gavahian, and M. Jalali, "Model-free adaptive fuzzy sliding mode controller optimized by particle swarm for robot manipulator," International Journal of Information Engineering and Electronic Business (IJIEEB), **5**, p. 68, (2013)
9. D. K. Pratihar, K. Deb, and A. Ghosh, "A genetic-fuzzy approach for mobile robot navigation among moving obstacles," International Journal of Approximate Reasoning, **20**, pp. 145-172, (1999)
10. F. Betin, A. Sivert, A. Yazidi, and G. A. Capolino, "Determination of scaling factors for fuzzy logic control using the sliding-mode approach: Application to control of a DC machine drive," Industrial Electronics, IEEE Transactions on, **54**, pp. 296-309, (2007)
11. S. Kang, I. Yoo, M. Shin, and S. Seo, "Accurate inter-vehicle distance measurement based on monocular camera and line laser," IEICE Electronics Express, **11**, pp. 20130932-20130932, (2014)
12. L. Cheng, B. E. Henty, D. D. Stancil, F. Bai, and P. Mudalige, "Mobile vehicle-to-vehicle narrow-band channel measurement and characterization of the 5.9 GHz dedicated short range communication (DSRC) frequency band," Selected Areas in Communications, IEEE Journal on, **25**, pp. 1501-1516, (2007)
13. M. Rohani, D. Gingras, V. Vigneron, and D. Gruyer, "A new decentralized Bayesian approach for cooperative vehicle localization based on fusion of GPS and inter-vehicle distance measurements," in Connected Vehicles and Expo (ICCVE), 2013 International Conference on, pp. 473-479, (2013)
14. P. Seiler, B. Song, and J. K. Hedrick, "Development of a collision avoidance system," Development, **4**, pp. 17-22, 1998
15. W. Zhang, O. Tsimhoni, M. Sivak, and M. J. Flannagan, "Road safety in China: analysis of current challenges," Journal of safety research, **41**, pp. 25-30, (2010)
16. L. Fan and E. M. Joo, "Design for auto-tuning PID controller based on genetic algorithms," in Industrial Electronics and Applications, 2009. ICIEA 2009. 4th IEEE Conference on, pp. 1924-1928, (2009)